ISSN 0469-4732

INSTITUTE OF PLASMA PHYSICS

NAGOYA UNIVERSITY

Resonance Absorption of ICRF Wave in Edge Plasma

Ryo Sugihara and Kaoru Yamanaka

(Received – June 9, 1987)

IPPJ- 836 July, 1987

RESEARCH REPORT

NAGOYA, JAPAN

Resonance Absorption of ICRF Wave in Edge Plasma

Ryo Sugihara

Institute of Plasma Physics, Nagoya University, Nagoya, Japan

and

Kaoru Yamanaka

The Institute of Vocational Training, Kanagawa Prefecture, Japan

Abstract

An edge plasma is shown to significantly absorb ICRF wave when a resonant triplet, a cutoff-resonance-cutoff triplet, is constructed in the evanescent region. Two-ion-component plasmas in a torus are considered though the plasmas are modeled by a slab in which the density changes linearly along the x-axis. The resonance is a perpendicular-ion-cyclotron resonance, i.e., an Alfven resonance, and is formed when the applied frequency ω is smaller than the local cyclotron frequency, at the edge of the antenna side, of the lighter species of ions. Roughly the absorption rate A_b is given by M^2 for $M^2 \gg S^2$ and S^4 for $S^2 \gg M^2$ where $M = k_y l$ and $S \cong k_z l$ and l is a scale length of the order of the plasma minor radius and k_y and k_z are the perpendicular and the parallel components of the wave vector. It is noted that the both quantities, M and S, readily become of the order of unity. Since A_b is not very sensitive to the density ratio of the two ion species, a few percent of impurities may cause a significant absorption. As the mass ratio of the two ion species comes close to unity the triplet forms readily. Therefore a D-T plasma seems to suffer more easily this kind of resonance absorption than a D-H plasma.

1. INTRODUCTION

Anomaly in the propagation of ICRF wave in the plasma edge region is one of main concerns in RF heating in relation to the efficiency of heating and to anomalous transports. It is reported that a significant fraction of the wave energy transfers to that of the coaxial mode and is trapped in the scrape-offlayer when ICRF wave or a compressiona Alfven wave is excited by a coupler or an antenna[1]. Parasitic excitation of ion Bernstein waves is also observed on the surface[2]. Excitation of a surface mode is pointed out as well[3]. The energy of the modes thus excited will be dissipated in the plasma surface, which results in lowering the heating efficiency. In addition the deposition of these wave energies on the plasma edge implies the heating of the plasma surface which may leads to a metal impurity production. Excitations of some of these harmful modes might be suppressed by modifying the design of the antenna[4-6].

In this paper we point out another serious problem relevant to the ICRF wave propagation in the plasma edge, i.e., a resonant absorption through an Alfven resonance in the evanescent region in the edge. Through the text torus plasmas, typically tokamak plasmas, are considered. For a single-ion-species plasma, there appears an Alfven resonance or the perpendicular-ion-cyclotron resonance when the applied frequency ω is smaller than the ion cyclotron frequency Ω. For this frequency the resonance will take place near the plasma edge of the torus plasma as seen in the next section. In reality the usual ICRF heating scheme uses two ion components. For the minority heating the minority ion concentration is much less than the majority one [7] while for the mode-conversion heating both densities can be comparable [8]. The frequency ω is set between the cyclotron frequencies of the two ion components. For these heating schemes the

resonance appears in the edge plasma as well as in the main plasma. This feature is clearly shown in a review paper by Perkins [9]. We claim in the present paper that for ICRF heating a significant absorption of the wave may take place near the plasma edge and may give rise to several deleterious effects on the plasma confinement.

The resonance region is composed of a R-cutoff, a resonance and a L-cutoff layers and usually looks like a crescent [9], where R- and L-cutoffs stand for the cutoffs for right and left hand polarized waves. This resonance was first discussed by Messiaen et al.[10], and succeedingly Karney et al.[11] quantitatively study the absorption using MHD model. They showed that a remarkable absorption occurs under some conditions even if the wavelength is much larger than the scale length of the density gradient. Their assumptions are that the plasma is composed of a single species of ion, the frequency is much less than the ion cyclotron frequency, the wave is incident upon the triplet from the propagation region or from the main plasma and reflects back to the propagation region. Also Donnelly et al. examined this resonance in detail in MHD [12] as well as in a kinetic frame work [13].

Here we treat the wave absorption at the Alfven resonance in a two-ion-species plasma, employing the technique of Karney et al.. The applied frequency ω is smaller than the cyclotron frequency of the lighter ion species and collisions are assumed negligible. The wave is supposed to be injected from the outside or launched by an antenna. Some fraction of the wave energy incident on the resonance will be absorbed and the rest will be transmitted to the propagation region or the main plasma.

MHD theory, including the Hall term but excluding plasma pressure effects, is used and we analytically obtain the absorption rate. The

assumption of ignorance of the pressure effects or the assumption of the collision-free plasma indicates that discussion on details of the mode-conversion which will take place at the resonance can not be done in this paper. We are only interested in any anomaly of the propagation of ICRF wave near the plasma edge arising from the triplet resonance. It should be, however, noted that the converted waves either progress inside the plasma when the electron temperature T_e is high enough or reflect back to the edge of the plasma when T_e is low [13]. This fact is also remarked in the paper by Winglee in which the ICRF wave propagation in the presence of the Alfven resonance in a multi-species plasma is dealt with in the WKB approximation and which will be a good reference to the present theory[14] .

It is noted that there are many kinds of the combination of the two -ion-species. In current experiments the combinations of D-H, and of D-^{3}He are most popular. In future experiments in which D and T are used, both heating schemes (minority heating and mode-conversion heating) can be utilized without adding any external ion species.

Extension of the theory to a plasma having more than two-ion- components will be trivial. One example of such plasmas is a D(majority)-T(majority)-^{3}He(minority) plasma which may be used in Compact Ignition Tokamak [15]. Also in a D-T plasma contaminated with protons there is a very fair possibility of the production of the crescents since the proton cyclotron frequency is higher than ω at the edge if $\omega \sim \Omega_d$, the duterium cyclotron frequency, or $\omega \sim \Omega_t$, the tritiumm cyclotron frequency. Once the crescents are formed the wave is absorbed there, heat the plasma surface, tends to desorb impurities continuously and may lead to the desruption of the plasma.

Our calculation treats two-ion-component plasmas ; the first component

is called " a"-ion species and the second is called " b"-ion species. The masses, the densities and the charges of these species are m_a, n_a, Z_a and m_b, n_b, Z_b, respectively. We assume that $Z_a/m_a < Z_b/m_b$. Namely, the b-ion species is " effectively " lighter than the a-ion species. The ratio n_b/n_a can be arbitrary. If $n_b/n_a \ll 1$, this is the case of the minority heating and, if $n_b/n_a \sim 1$, this is the case of the mode-conversion heating.

The plan of this paper is following. In section 2 we give an overview of the resonance and cutoff lines in the minor cross section in a torus. Especially we emphasize those in the plasma edge. In section 3 we analyse the wave behavior in the presence of the resonance triplet or the crescent, essentially employing the technique in Ref.11. The analysis will be done on the slab model, and in some limits we will give explicit solutions. The most important thing is that there comes out a scale length which is usually much smaller than the vacuum wavelength and much larger than the density scale length and which governs the wave propagation in the plasma edge. In section 4 the definition of wave absorption at the triplet will be given and analytical formulations in some limits are shown. In section 5, a more detailed estimation will be done on the wave absorption by using numerical computations and the solutions will be compared with the analytical ones. Discussion is given in section 6 on the validity of the model, of the calculations and on the relevance to actual fusion plasmas and so on. Finally conclusions will be given in section 7.

2. GEOMETRY OF RESONANCE AND CUTOFF LINES

For a while we assume that the characteristic length of the density gradient is so long compared with the wavelength that the WKB approximation be applied to. Then the dispersion relation will be given by

$$k_\perp^2 = (A - D)(A + D)/A, \tag{1}$$

$$A = k_0^2 - k_z^2 + k_0^2\left(\frac{\Pi_e^2}{\Omega_e^2} - \frac{\Pi_a^2}{\omega^2 - \Omega_a^2} - \frac{\Pi_b^2}{\omega^2 - \Omega_b^2}\right), \tag{2}$$

$$D = k_0^2\left(\frac{\Pi_e^2}{\omega|\Omega_e|} + \frac{\Pi_a^2\Omega_a}{\omega(\omega^2 - \Omega_a^2)} + \frac{\Pi_b^2\Omega_b}{\omega(\omega^2 - \Omega_b^2)}\right),$$

$$= k_0^2\left(\frac{\omega\Pi_a^2}{\Omega_a(\omega^2 - \Omega_a^2)} + \frac{\omega\Pi_b^2}{\Omega_b(\omega^2 - \Omega_b^2)}\right), \tag{3}$$

where $k_0 = \omega/c$ and Π_j and Ω_j are the plasma and the cyclotron frequencies of the j-th species and the subscript j stands for e(electron), a and b. The k_z and $k_\perp$ are the wave vector components along and perpendicular to the magnetic field, respectively. Using the dispersion relation (1), we survey the geometries of resonance and cutoff lines on cross sections of torus plasmas.

The surface where

$$A = 0 \tag{4}$$

defines the ion-ion hybrid resonance in the propagation region or in the main plasma. In the evanescent region Eq.(4) also yields the Alfven resonance or the perpendicular-ion-cyclotron resonance(PICR) which is our main concern. The usual fast magnetosonic cutoff is given by $A - D = 0$. The surface $A + D = 0$ is a cutoff that occurs near the ion-ion hybrid resonance. This cutoff also occurs near PICR in the evanescent region and produces the

cutoff-resonance-cutoff triplet or the crescent. In Fig.1 the resonances and the cuoffs for a single-ion-species plasma are depicted.

Fig.1

No ion-ion hybrid resonance, of course, occurs but, as shown in Figs.1(b) and 1(c), PICR does in the evanescent region which is treated in Ref.11. In Fig.2 a two-ion-species plasma is considered.

Fig.2

These geometries may be commonly realized in D-H, D-^{3}He and D-T plasmas and are mainly concerned in this paper. We note that Figs.2(a) and 2(e) are topologically and also physically equivalent to Figs.1(a) and 1(c), respectively. The configuration shown in Fig.2(b) is usually utilized in ICRF mode-conversion heating. Figure 3 represents a specific example for a three-ion-species plasma.

Fig.3

Such configuration could take place when small amount of hydrogen or ^{3}He is mixed up for the minority heating of a D-T plasma or when hydrogen impurity is desorbed from the wall. Other examples of the cross sectional view are given in Ref.9. In general, the crescents are easy to form as the aspect ratio is reduced and/or the mass ratio of the two-ion- species comes near unity. Therefore the crescents in the D-T plasma may be more easily created than in a D-H plasma.

The discussion in this section has been done on the basis of WKB approximation. In actual plasmas, the situation will be somewhat different, i.e., the wavelength must be longer than the scale length of the density gradient and therefore Figs.1-3 only contribute to giving us a rough image of the nature of the wave in those cross sections. Nevertheless, these figures indicate that, at least, singularities to the wave propagation exist in the rare plasma around the plasma edges for a proper set of parameters. In the next section analytic treatments will be developed on the behavior of the wave near the plasma boundary.

3. ANALYSIS

To analyze the ICRF wave propagation in the edge plasma we introduce the following model. The plasma is composed of two-ion species. Since the consideration is restricted within a narrow region around the edge the plasma is approximated by a one-dimensional slab plasma in which the density changes linearly along the x-axis and a uniform magnetic field directs to the z-axis. The crescents in this model become infinitely long in the direction of the y-axis; the relevance to actual situations will be discussed in section 6. The antenna current flows along the y-axis and its amplitude is assumed constant. In this model we can write the oscillating quantities as $f(x,y,z,t) = g(x)\exp i(k_y y + k_z z - \omega t)$ and can choose k_0, k_y and k_z arbitrarily. However, throughout this paper we take $k_0^2 - k_z^2 < 0$ since this is most realistic in the current experiments while k_y will be taken arbitrarily. A schematic diagram of the system we are considering is depicted in the upper half of Fig.4 and the dispersion relation is shown in the lower half.

Fig.4

The dispersion curve still results from the WKB approximation and now k_x^2 is the variable instead of k_i^2 ($= k_x^2 + k_y^2$).

In deriving the wave equations we assume that $E_z = 0$ because of the large dielectric tensor element ε_{zz}, that no thermal effect is included and that the plasma exists in $x > 0$. The resultant wave equations are

$$(A - k_y^2)E_x - i(D + k_y d/dx)E_y = 0, \tag{5}$$

$$i(D - k_y d/dx)E_x + (A + d^2/dx^2)E_y = 0. \tag{6}$$

They are reduced to a coupled set of first order differential equations,

$$(d/dx)E_y + (k_y D/A)E_y = \{(A - k_y^2)/A\}\psi, \tag{7}$$

$$(d/dx)\psi - (k_y D/A)\psi = -\{(A^2 - D^2)/A\}E_y, \tag{8}$$

where $\psi = -c^{-1}\partial B_z/\partial t$. Note that for $x < 0$ we have $A = k_0^2 - k_z^2$ and $D = 0$. Equations (7) and (8) are the same as Eqs.(4) and (5) in Ref.11 though the present A and D are quite different from those in the reference. As is seen in the above set the field becomes singular at a point where Eq.(4) holds and we anticipate that the wave be absorbed around the singular point. The two equations (7) and (8) are easily unified to be

$$\frac{d^2}{dx^2}E_y + \left(\frac{d}{dx}ln\frac{A}{A - k_y^2}\right)\frac{d}{dx}E_y +$$

$$+ \left(\frac{A - k_y^2}{A}\frac{d}{dx}\left(\frac{k_y D}{A - k_y^2}\right) + \frac{A^2 - D^2 - Ak_y^2}{A}\right)E_y = 0. \tag{9}$$

It is noted that when the plasma is uniform the dispersion relation (1) is reproduced from (9).

We have assumed a linear density gradient which is represented by

$$n_j(x) = n_{j0}x/d. \tag{10}$$

(The explicit values of the edge density n_{j0} and the scale length d will be discussed in section 6.) Hence $A(x)$ and $D(x)$ can be written as

$$A(x) = k_0^2 - k_z^2 - k_0^2(x/d)A_0, \tag{11}$$

$$D(x) = k_0^2(x/d)D_0, \tag{12}$$

where A_0 and D_0 are defined by

$$A_0 = -\Pi_{e0}^2/\Omega_e^2 + \Pi_{a0}^2/(\omega^2 - \Omega_a^2) + \Pi_{b0}^2/(\omega^2 - \Omega_b^2), \tag{13}$$

$$D_0 = (\omega\Pi_{a0}^2/\Omega_a)/(\omega^2 - \Omega_a^2) + (\omega\Pi_{b0}^2/\Omega_b)/(\omega^2 - \Omega_b^2), \tag{14}$$

and the densities in the plasma frequencies, Π_{j0}, are constant and are n_{j0}. For convenience we introduce density ratios, $(\eta_{ab}, \eta_{ba}) = (Z_a n_{a0}, Z_b n_{b0})/(Z_a n_{a0} + Z_b n_{b0}) = (Z_a n_{a0}, Z_b n_{b0})/n_{e0}$. It is supposed that $A(x)$ takes zero at $x = x_0$, i.e.,

$$A(x_0) = k_0^2 - k_z^2 - k_0^2(x_0/d)A_0 = 0, \tag{15}$$

or

$$A(x) = (x - x_0)\cdot(d/dx)A(x_0)$$

$$= -k_0^2(x - x_0)A_0/d. \tag{16}$$

We note that A_0 must be negative in order that the resonance point is inside the plasma or x_0 is positive since $k_0^2 - k_z^2$ has been assumed negative.

We here introduce a new scale length l defined by

$$l = | (d/dx)A(x_0) |^{-1/3} = | k_0^2A_0/d |^{-1/3}, \tag{17}$$

which is also written as

$$l = [x_0/(k_z^2 - k_0^2)]^{1/3}, \tag{18}$$

with the help of (15). The l is the most important scale length in this theory and in a typical tokamak plasma the relation

$$k_0^{-1} \gg r_p \gtrsim l \gg d, \tag{19}$$

holds where r_p is the minor radius of the tokamak plasma. Hereafter x is scaled with l as

$$\xi = (x - x_0)/l, \tag{20}$$

and then

$$A(x) = \xi/l^2, \tag{21}$$

$$D(x) = -\xi h/l^2 - \xi_0 h/l^2, \tag{22}$$

$$h = D_0/A_0, \tag{23}$$

$$\xi_0 = x_0/l. \tag{24}$$

Here we define an important parameter S by

$$S = l(k_z^2 - k_0^2)^{1/2}, \tag{25}$$

which is related to ξ_0 as

$$\xi_0 = S^2,$$

where (18) and (24) were used. Now Eq.(9) reduces to

$$\frac{d^2}{d\xi^2}E_y - \frac{M^2}{\xi(\xi - M^2)}\frac{dE_y}{d\xi} + \{\frac{F}{\xi(\xi-M^2)} - \frac{G^2}{\xi} - H + I\xi\}E_y = 0, \tag{26}$$

where

$$M = k_y l,\ F = -Mh(S^2 + M^2),\ G = hS^2,\ H = 2h^2S^2 + M^2,\ I = 1 - h^2.$$

It is supposed that $|h|$ is at most unity. It seems that in Eq.(26) there are two singular points, i.e., $\xi = 0$ and $\xi = M^2$. However, the true singular point is $\xi = 0$ while $\xi = M^2$ is an apparent singular point. This fact is inferred from (7) and (8) and has been pointed out[16], and hence we pay attention to the former singular point.

We try to solve (26) analytically. It is supposed that the ICRF wave is incident from the negative ξ side , passes through the triplet and is transmitted into the positive ξ or the propagation region.

In the limit of $\xi \to \infty$, eq.(26) becomes

$$\frac{d^2}{d\xi^2}E_y + (I\xi - H)E_y = 0. \tag{27}$$

The solution to this equation is given by a linear combination of the Airy's functions $A_i(-\zeta)$ and $B_i(-\zeta)$, ζ being

$$\zeta = I^{1/3}(\xi - H/I).$$

Because the wave for $\xi >> 1$ must be a traveling wave, the solution should have the form of

$$E = iA_i(-\zeta) + B_i(-\zeta) \tag{28}$$

$$\sim [\pi^{1/2}(1.5\zeta)^{1/6}]^{-1} \exp(i\zeta + i\pi/4). \tag{29}$$

Next we look for solutions valid around $\xi = 0$. Now it is convenient to treat cases separately.

Case I. $1 \gg M^2 \gg S^2$.

In the vicinity of the resonance point $\xi = 0$ the relation $|\xi| << 1$ holds and we may have the solution to Eq.(26) in a form of ascending series of ξ. For $\xi > 0$, a solution will be

$$E_1 = 1 + a_1\xi + a_2\xi^2 + , \tag{30}$$

where the first two of the coefficients a_i are given by

$$a_1 = F/M^2 + G^2 \ , \tag{31}$$

$$a_2 = [a_1^2 + (H - G^2/M^2)]/4. \tag{32}$$

The other solution will be given by

$$E_2 = M^2 E_1 \ln \xi + b_1 \xi + b_2 \xi^2 + \ , \tag{33}$$

where

$$b_1 = -(1 + 2a_1 M^2), \tag{34}$$

$$b_2 = -M^2 a_1^2/2. \tag{35}$$

The appropriate combination of E_1 and E_2 that matches onto Eqs. (28) or (29) in the region $M^2 << \xi << 1$ is

$$E_y = \alpha_1 E_1 + \beta_1 E_2, \tag{36}$$

$$\alpha_1 = (i + 3^{1/2}) c_1 - (i - 3^{1/2}) c_2 H/I^{2/3}, \tag{37}$$

$$\beta_1 = [(i - 3^{1/2}) c_2 I^{1/3} - a_1 \alpha_1]/b_1, \tag{38}$$

where $c_1 = A_i(0) = 0.335$ and $c_2 = -(d/dx)A_i(0) = 0.259$ and

$$c_1 c_2 = (2 \cdot 3^{1/2} \pi)^{-1}. \tag{39}$$

We may obtain the wave field in the region of $\xi < 0$ by analytically continuing the solution (36) into that region , bearing in mind that causality requires us to go above the singularity at $\xi = 0$ in the complex plane. Therefore the solution will be, for $\xi < 0$,

$$E_y = \alpha_1 E_1 + \beta_1 E_{2r} + i\pi\beta_1 E_{2i}, \tag{40}$$

$$E_{2r} = M^2 E_1 \ln|\xi| + b_1\xi + b_2\xi^2 + , \tag{41}$$

$$E_{2i} = M^2 E_1. \tag{42}$$

Thus the solution available over $-\xi_0 < \xi < \infty$ is obtained.

Case II. $S^2 \ll 1$ and $M^2 = 0$.

We should treat the case of $1 \gg S^2 > M^2$ ($\neq 0$) in order to compare to Case I. However, keeping M^2 finite gives us a severe difficulty in the analysis. Hence we choose $M^2 = 0$. The governing equation now reduces to

$$\frac{d^2}{d\xi^2}E_y + (-\frac{G^2}{\xi} - H + I\xi)E_y = 0. \tag{43}$$

This equation has a singular point at $\xi = 0$, is very similar to the Budden equation [17] and then an absorption is expected. Actually this type of equation has been solved and a significant wave absorption has been shown to take place [18]. We solve this equation again by using an ascending series of ξ. The same symbols as those used in Case I will be used as long as they cause no confusion. We see the two solutions be given by

$$E_1 = \xi + (G^2/2)\xi^2 + \ , \tag{44}$$

$$E_2 = G^2 E_1 ln\xi + 1 + (G^2/2)\xi + (H - G^4)\xi^2/2 + \ . \tag{45}$$

That they are the solutions to Eq. (43) will be ascertained by inserting (44) and (45) into (43). The appropriate combination of E_1 and E_2 that matches onto Eq. (28) in the region $M^2 \ll \xi \ll 1$ is

$$E_y = \alpha_2 E_1 + \beta_2 E_2, \tag{46}$$

where

$$\alpha_2 = (i - 3^{1/2})c_2 I^{1/3} - G^2(i + 3^{1/2})c_1/2, \tag{47}$$

$$\beta_2 = (i + 3^{1/2})c_1 - (i - 3^{1/2})c_2 I^{-2/3} H. \tag{48}$$

After the analytical continuation, we get the solution for $\xi < 0$ in the form

$$E_y = \alpha_2 E_1 + \beta_2 E_{2r} + i\pi\beta_2 E_{2i}, \tag{49}$$

$$E_{2r} = G^2 E_1 ln|\xi| + 1 + (G^2/2)\xi + , \tag{50}$$

$$E_{2i} = G^2 E_1. \tag{51}$$

Thus again the solution available over $-\xi_0 < \xi < \infty$ for $S^2 \ll 1$ and $M^2 = 0$ is obtained.

4. ENERGY ABSORPTION AT THE TRIPLET

We will evaluate the wave absorption at the resonance without regard to detailed mechanisms of the absorption; discussions on this point will be given in the next section.

In order to specify the amount of the absorbed power we notice the following fact. The radiation power density W from the antenna is given by a time-average of the product of the antenna current density $\vec{J}$ and the local electric field $\vec{E}$, that is,

$$W = -<\vec{E}\cdot\vec{J}>, \tag{52}$$

where $<\ >$ denotes the time-average. From the energy conservation law of the electromagnetic wave we see that the difference between W and $P(\infty)$, the Poynting flux at $\xi \to \infty$, will give us the wave absorption in the plasma. Meanwhile the Poynting flux at the plasma edge $\xi = -\xi_0$,

$$P(-\xi_0) = (c/4\pi)Re(E_y B_z^*/2), \tag{53}$$

may be equal to W because in vacuum between the antenna and the edge no energy loss is expected, where X^* indicates the complex conjugate of X and $Re(X)$ denotes the real part of X. Therefore we define the absorpton rate A_b by

$$A_b = 1 - \frac{P(\infty)}{P(-\xi_0)}. \tag{54}$$

First we evaluate $P(\infty)$. From (5) we have

$$E_x = i\{DE_y + k_y(d/dx)E_y\}/(A - k_y^2). \tag{55}$$

Using (55) and the induction law of the Maxwell equations we have

$$ik_0B_z = (k_yDE_y + A(d/dx)E_y)/(A - k_y^2). \tag{56}$$

Referring to the definition of $A(x)$ in (21) and $D(x)$ in (22), we get at $\xi \to \infty$,

$$ik_0B_z = l^{-1}(d/d\xi)E_y - hk_yE_y.$$

Now the Poynting flux $P(\infty)$ will be given by

$$P(\infty) = (c/4\pi)Re[(E_yB_z^*)/2] \tag{57}$$

$$= -(c/8\pi k_0 l)Im[E_y(d/d\xi)E_y^*], \tag{58}$$

since the cold plasmas have been assumed[13] where $Im(X)$ indicates the imaginary part of X. Using (28) or (29), we easily get

$$P(\infty) = cI^{1/3}/(8\pi^2 k_0 l). \tag{59}$$

The $P(\infty)$ has the dimension of velocity because the non-dimensional $\vec{E}$ and $\vec{B}$ have been used in (57). Since only the ratio $P(\infty)/P(-\xi_0)$ is needed, however, we do not adhere to the dimension of the flux P.

The algebra for getting $P(-\xi_0)$ is a little complicated. The E_y and $dE_y/d\xi$ in Case I are different from the corresponding ones in Case II. Then we treat them separately as before.

Case I. $1 \gg M^2 > S^2$.

In the limit of $\xi \to -\xi_0$, i.e., $x \to 0$ and $n_j \to 0$, Eq. (56) becomes

$$ik_0 B_z = \frac{k_z^2 - k_0^2}{k_y^2 + k_z^2 - k_0^2}\cdot\frac{dE_y}{dx},$$

and hence, following (57), $P(-\xi_0)$ is given by

$$P(-\xi_0) = -\frac{c}{8\pi k_0 l}\cdot\frac{k_z^2 - k_0^2}{k_y^2 + k_z^2 - k_0^2}\cdot Im(E_y\frac{dE_y^*}{d\xi}), \tag{60}$$

where E_y and $(d/dx)E_y^*$ are of course the values at $\xi = -\xi_0$. Using (40), (41) and (42), we have

$$Im[E_y(d/d\xi)E_y^*] = Y_1\cdot Y_2, \tag{61}$$

where Y_1 and Y_2 are expressed as

$$Y_1 = Im(\alpha_1^*\beta_1) - \pi M^2|\beta_1|^2,\quad Y_2 = E_{2r}(d/d\xi)E_1 - E_1(d/d\xi)E_{2r}.$$

By use of (37) and (38), Y_1 reduces to

$$Y_1 = -I^{1/3}/(\pi|b_1|) - 4\pi M^2(c_2^2 I^{2/3} + a_1c_1c_2 I^{1/3} + a_1^2c_1^2)/b_1^2. \tag{62}$$

Also Y_2 reduces to

$$Y_2 = -b_1 + M^2/\xi_0 - 2a_1M^2 + 2b_2\xi_0 + O(\xi_0^2)$$

$$= \frac{k_y^2 + k_z^2 - k_0^2}{k_z^2 - k_0^2} + 2b_2\xi_0 + \ , \tag{63}$$

where use has been made of (25), (34) and $M^2 = k_y{}^2l^2$. Now combining (60), (61), (62) and (63), and collecting quantities up to $O(M^2)$, we get

$$P(-\xi_0) = cI^{1/3}/(8\pi^2 k_0 l) + (cI^{1/3}/8\pi^2 k_0 l) M^2 W_1, \tag{64}$$

$$W_1 = 4\pi^2[c_2^2 I^{1/3} + a_1 c_1 c_2 (1 - \frac{1}{2\pi^2 c_1 c_2}) + a_1^2 c_1^2 I^{-1/3}]. \tag{65}$$

Referring to (59), we see that the first term on RHS of (64) indicates the transmitted power and then the second term signifies the absorption power in the plasma. Thus it is found that

$$A_b = M^2 W_1. \tag{66}$$

Now it is understood that the absorption is in proportion to M^2 or k_y^2 in the case of $1 \gg M^2 > S^2$.

Case II. $S^2 \ll 1$ and $M^2 = 0$.

In this case, $P(-\xi_0)$ is just written as

$$P(-\xi_0) = -(c/8\pi k_0 l) Im[E_y (d/d\xi) E_y^*] . \tag{67}$$

Again we write

$$Im[E_y (d/d\xi) E_y^*] = Y_1 \cdot Y_2,$$

where Y_1 and Y_2 are expressed as

$$Y_1 = Im(\alpha_2^* \beta_2) - \pi G^2 |\beta_2|^2, \quad Y_2 = E_{2r} (d/d\xi) E_1 - E_1 (d/d\xi) E_{2r}.$$

Use of (47), (48) and (39) reduces Y_1 to

$$Y_1 = -(2 \cdot 3^{1/2} c_1 c_2 I^{1/3} + 4\pi G^2 c_1^2)$$

$$= -(I^{1/3}/\pi)(1 + 4\pi^2 c_1^2 G^2 I^{-1/3}).$$

Meanwhile, by use of (44), (50) and (51), Y_2 reduces to

$$Y_2 = 1 + G^4\xi_0^2 \ln|\xi_0| + G^4\xi_0^2/2 + .$$

Collecting quantities up to $O(G^2)$ or $O(S^4)$ and using the definition of A_b, (54), we get,

$$A_b = 4\pi^2 G^2 c_1^2 I^{-1/3} \tag{68}$$

$$= 4\pi^2 c_1^2 h^2 S^4 I^{-1/3}. \tag{69}$$

5. NUMERICAL SOLUTIONS

It is noted that the governing equation (26) depends on only three parameters, h, M and S as being manifest from the definitions of F,G,H and I. First, we solve (26) numerically in the $M - S(>0)$ space. The boundary condition which is consistent with the analytical calculation is that the solution should agree with the traveling wave solution (28) or (29) in the propagation region. Near $\xi = 0$, ω is replaced with $\omega + i\nu$ so that the psuedo-collision term ν removes the singularity. We have confirmed that, provided that $\nu \ll \omega$, the power absorbed is independent of ν, and therefore we regard the power as the absorbed one. The computed rates for $h = 0.2$, 0.5 and 0.8 are shown in Fig.5 by contour lines.

Fig.5

The curves are asymmetric in the axis of $M = 0$. This reflects the asymmetry of the coefficient F. Also the analytical values which are evaluated by using (66) and (69) are given on the horizontal and the vertical axes. When $|M| \lesssim 0.3$ and $S = 0$, A_b in (66) reproduces the numerical value fairly well. Also when $S \lesssim 0.3$ and $M = 0$, A_b in (68) or (69) agrees with the numerical value quite well. Referring to these results and to Figs.5(a), 5(b) and 5(c), we may conclude that the analytical expression (66) well approximates A_b for $|M| \lesssim 0.3$ and $S \lesssim 0.1$ and that (68) or (69) is valid for $S \lesssim 0.3$ and $|M| \lesssim 0.1$. It is noted that even when $|M| \sim 1$ and $S \lesssim 0.1$ and when $S \sim 1$ and $|M| \lesssim 0.1$ the discrepancies are not appreciable.

Equation (69) implies that A_b for $M = 0$ is strongly dependent on h, the ratio D_0/A_0. As $|h|$ approaches unity, the quantity $I = 1 - h^2$ tends to zero, the evanescent region becomes infinitely broad as Eq.(27) indicates and the wave coming onto the resonance may be perfectly absorbed as implied in Ref.17. We estimate the h-dependence of A_b for a fixed l, which implies that D_0 is changed under a fixed A_0. Numerical results for $S = 0.2$, 0.5 and 0.8 are given in Fig.6.

Fig.6

The curves are symmetric upon the point $M = 0$ and $h = 0$, which reflects the same symmetry of the coefficients in Eq.(26). The analytical and the numerical curves well agree with each other almost independently of S value when $|h| \ll 1$ and $|M| \ll 1$ or more explicitly when $|h| \lesssim 0.3$ and $M \lesssim 0.5$.

The good agreement between the analytical and the numerical values

exhibited in Figs.5 and 6 implies that the expressions (66) and (69) are very useful and sometimes give exact values when estimating the wave absorption.

6. DISCUSSION

The dependence of A_b on the density ratio η_{ab} or η_{ba} is one of main concerns in this study. The absorption necessitates the presence of resonances which are governed by $A(x)$. The $A(x)$ as seen in (2) satisfies the resonance condition $A(x) = 0$ for any small η_{ba} if ω is adjusted properly. In this sense an appreciable absorption can be expected for any small η_{ba} which corresponds to a minority heating and also to an impurity contamination.

We have assumed a collision-free plasma and the wave is supposed to mode-convert to some other waves. In the boundary plasma the temperature is relatively low and the converted waves may reflect back to the plasma edge [26]. This means that the wave energy may pile up in the edge and convert to thermal energy through rare collosions and/or some non-linear processes. The locally heated surface enhances impurity production and also may give rise to some kind of convections which result in an anomalous plasma transport.

The infiniteness of the length of the crescent along the y-axis makes the present model different from actual plasmas in which the length is finite. However, the model may be valid if the antenna spectrum has components $k_y > 1/l_c$ and M is not vanishingly small for such k_y where l_c is the length of the crescent in an actual plasma. In this case there must be a significant absorption to such spectrum components.

We here consider the edge profile. The scale length d of the density gradient in the edge for most plasmas except for H-mode ones [19] is probably

much larger than that of the steepest gradient in the main plasma and is plausibly assumed to be of the order of the plasma radius r_p. In order for $A(x)$ to have a zero point near the edge the edge density n_{j0} in (10) is so low that

$$\Pi_{\alpha 0}^2 \sim n_z^2|\omega^2 - \Omega_\alpha^2| \sim n_z^2\Omega_\alpha^2,$$

is satisfied. Suppose that "α"-ion species is deuterium, the magnetic field is 5 tesla and that n_z^2 is several tens, then n_{j0} is of the order of 10^{12} cm^{-3}. The values of $d \sim r_p$ and $n_{j0} \sim 10^{12}cm^{-3}$ will not be inconsistent to those of current tokamak plasmas. Therefore the resonance absorption so far considered will plausibly occur in actual tokamak plasmas.

It can be shown that the D-T plasma tends to be accompanied with large and broad crescents compared with those in the D-H plasma because in the former the mass and the density ratios are more close to unity than those in the latter : Usually in the D-H plasma, H is mixed up as a minority for the sake of the heating while in the D-T plasma the ratio η_{td} or η_{dt} can be arbitrary. Another comment as to the crescents in the D-T plasma is that in the transition from the starting phase to the steady burning phase the ratio η_{td} or η_{dt} may change drastically, the sizes of the crescents do change, too, and unexpectedly strong absorptions might occur around the plasma edge during the operation of the fusion reactor. In such case a huge heat deposit near the plasma boundary may take place and may lead to destruction of the first wall.

When we apply the present theory to an actual situation we should first draw the cross sectional view of the resonance and the cutoff similar to Figs.1-3 and if we find any crescent around the edge we must estimate M

and S. If one of M and S or the both are not too small there is a fear of significant edge absorption. Now M and S are explicitly estimated by using parameters of a typical tokamak plasma. We choose $x_0 = 0.1r_p$, $|k_y| = r_p^{-1}$ and $k_z = s/R$, where R is the major radius of the tokamak plasma and s is the toroidal mode number. In order to determine the scale length l we use (18) and assume $k_z^2 \gg k_0^2$. Therefore l is given by $(x_0/k_z^2)^{1/3} = (0.1r_pR^2/s^2)^{1/3}$. Then for a tokamak of its aspect ratio $R/r_p = 4$, $|M|$ and S become $1.2s^{-2/3}$ and $0.3s^{1/3}$, which are of the order of unity. In this case, as Fig.5 implies, the ICRF wave may be significantly absorbed in the triplet if $|h| < 1$.

7. CONCLUSIONS

ICRF wave absorption in edge regions of two-ion-component plasmas is considered. The plasmas are modeled by a slab and are assumed cold and collision-free. The wave injected from the outside is strongly absorbed at a triplet layer, i.e., a cutoff-resonance-cutoff layer. The absorption rates are evaluated analytically in some limits and are computed numerically. Such triplet or a crescent can be constructed when the applied frequency is less than the local cyclotron frequency of the lighter constituent ion at the edge of the antenna side.

We now list some general comments and a summary of our results.

1. The formalism can be used for a two-ion-species plasma having an arbitrary constituent of ions and a density ratio of the corresponding ion species. Extension to a plasma with ion components more than two is trivial.

2. The theory is governed by a scale length l which is usually much larger than the scale length of the density gradient but much smaller than the vacuum wave length. In general, if $M = k_y l$ and/or $S = l(k_z^2 - k_0^2)^{1/2}$ are

not much small, there is a fear of significant absorption.

3. The appearance of crescents is governed by the density ratio η_{ab} or η_{ba} and their scale also depends on the ratio. Once the crescent is formed, however, the absorption rate is not very sensitive to η_{ab} or η_{ba}.

4. The theory assumes collision-free plasmas and therefore the absorption rates evaluated is equivalent to the rates of mode-conversion, the nature of which is not specified in the text. Since the temperature near the plasma boundary is low, the converted wave reflects back to the edge and may heat there through a rare collision and/or some non-linear processes. The surface heating may cause an enhanced impurity production or a plasma convection leading to anomalous transports.

5. Although the model is a slab in which the length of a crescent along the y-axis is infinite, the theory suggests that if the length of the crescent l_c in an actual plasma is such that $|k_y l_c| \gtrsim 1$ we may expect a significant absorption.

6. The crescents are harder to form in the H-mode plasma than in the L-mode plasma because of the steep gradient of the density at the surface in the former.

7. Generally, a D-T plasma is inclined to have wider and longer crescents than those in a D-H plasma. Moreover, in the D-T plasma the ratio η_{td} or η_{dt} can be arbitrary (but less than unity) and hence resonances near the edge take place more easily. Therefore the D-T plasma seems to more readily suffer this kind of resonance absorption.

8. The second harmonic heating of deuterium cyclotron frequency probably encounters a serious problem if the plasma is contaminated with hydrogen. Also light impurities may generate unexpected crescents in the edge and these crescents may also be harmful to the plasma confinement.

ACKNOWLEDGEMENTS

The authors are indebted for stimulating discussions to the colleagues of the workshop of theory and simulation of RF heating supported by the Grant-in-Aid for Fusion Research of the Ministry of Education, Science and Culture.

One of the authors (R. S.) would like to express his appreciation for the hospitality of Plasma Physics Group in Riso National Laboratory where a part of this work has been done.

REFERENCES

[1] BHATNAGAR, V.P., EVRARD M.P., FAULCONER, D.W., GEILFUS, P., KOCH, R., LUWEL, M., MESSIAEN, A.M. PEASON, D.I.C., VANDENPLAS, P.E., WEYNANTS, R.P., in Plasma Physics and Controlled Nuclear Fusion Research (Proc. 9-th Int. Conf. Baltimore, 1982) II, IAEA, Vienna (1983) 103.

[2] SKIFF, F., ONO, M., COLESTOCK, P., WONG, K.L., Phys.Fluids 28 (1985)2453.

[3] CRAMER, N.F., YUNG, C.-M., Plasma Phys. Contr. Fusion 28 (1986)1043.

[4] MORI, M., et al., in Plasma Physics and Controlled Nuclear Fusion Research (Proc. 10-th Int. Conf. London, 1984) I, IAEA, Vienna (1985) 445.

[5] TAYLOR, R.J., EVANS, J., KELLER, L., LAI, K.F., ROSSING, V., CASAVANT, T., KORTWABI, D., PRAGER, S.C., SPROTT, J.C., WITHERSPOON, F.C., ZHU, S.Y., in plasma Physics and Controlled Nuclear Fusion Research (Proc. 9-th Int. Conf. London, 1984) I, IAEA, Vienna (1985)581.

[6] OHKAWA, T., ANDREWS, P.L., HINO, T., CHAN, V.S., CHIU, S.C., IEEE Plasma Sci. PS-14 (1985) 563.

[7] STIX, T.H., Nucl. Fusion 15 (1975)737.

[8] SWANSON, D.G., Phys. Rev. Lett. 36 (1976) 316.

[9] PERKINS, F.W., Nucl. Fusion 17 (1977) 1197.

[10] MESSIAEN, A.M., WEYNANTS, R.R., BHATNAGAR, V.P., BURES, M., VANDENPLAS, P.E., Proc. 1st Joint Varenna-Grenoble Int. Symposium on Heating in Toroidal Plasmas, 1978, Grenoble, p.229.

[11] KARNEY, C.F.F., PERKINS, F.W., SUN, Y.-C., Phys, Rev. Lett. 42 (1979)1621.

[12] DONNELY. I.J., CLANCY. B.E., CRAMER. N.F., J. Plasma Phys., 34 pt.2 (1985) 227.

[13] DONNELY. I.J., CLANCY. B.E., CRAMER. N.F., J. Plasma Phys., 35 pt.1 (1986) 75.

[14] WINGLEE. R.M., Plasma Phys. and Controlled Fusion, 26 (1984) 511.

[15] SCHMIDT. J., BATEMAN. G., BLACKFIELD. D., et al., in Plasma Phys. & Controlled Nucl. Fusion Res., (Proc. 11th Int. Conf. Kyoto, 1986) H-I-2.

[16] APPERT, K., GRUBER, R., VACLAVIK, J., Phys. Fluids 17 (1974)1471.

[17] BUDDEN, .K.G., Radio Waves in the Ionosphere, Cambridge University Press, Cambridge (1961)476.

[18] SUGIHARA, R., J. Phys. Soc. Jpn, 27 (1966)786.

[19] WAGNER. F., BECKER. G., BEHRINGER. K., et al., Phys. Rev. Lett. 49 (1982) 1408.

Figure Captions

Fig.1 Schematic description of resonances and cutoffs for a single-ion-species plasma on a minor cross section of a torus with a circular cross section. The wave is resonant on the line S on which $A = 0$. The label R(L) is the cutoff for a right (left) hand polarized wave. HFS stands for " high field side". a) The resonance $\omega = \Omega_a$ is in HFS outside the plasma, b) $\omega = \Omega_a$ inside the plasma, c) $\omega = \Omega_a$ in LFS (low field side) outside the plasma.

Fig.2 Schematic description of resonances and cutoffs for a two-ion-species plasma. a) Resonances $\omega = \Omega_a$ and $\omega = \Omega_b$ are both in HFS outside the plasma, b) $\omega = \Omega_a$ is in HFS outside the plasma while $\omega = \Omega_b$ is inside the plasma, c) Both $\omega = \Omega_a$ and $\omega = \Omega_b$ are inside the plasma, d) $\omega = \Omega_a$ is inside the plasma while $\omega = \Omega_b$ is in LFS outside the plasma, e) Both $\omega = \Omega_a$ and $\omega = \Omega_b$ are in LFS outside the plasma.

Fig.3 An example of the complexed resonances and cutoffs for a three-ion-species plasma.

Fig.4 Model for the calculation. The z-axis is along the magnetic field B_0. The dispersion curve based on the WKB approximation is depicted in the lower part.

Fig.5 Absorption rate A_b in M-S space. The solid curves are given by a numerical computation and the closed circles and the crosses are obtained by using (66) and (69), respectively. a) $h = 0.2$, b) $h = 0.5$, c) $h = 0.8$.

Fig.6 Absorption rate A_b in M-h space. The A_0 is fixed and only D_0 is changed. The solid lines show the numerical values and the chained lines are the values obtained by using (66). The curves are symmetric

upon the point $M = 0$ and $h = 0$. a) $S = 0.2$, b) $S = 0.5$, c) $S = 0.8$.

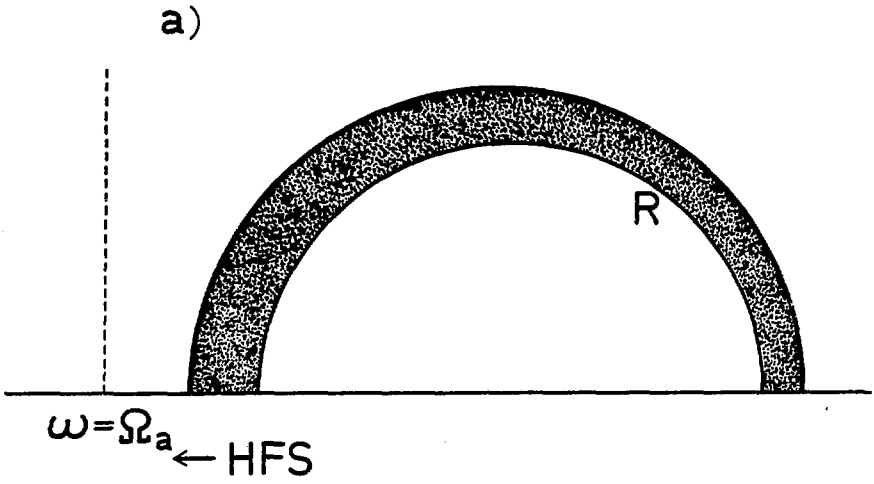

FIG.1(a)

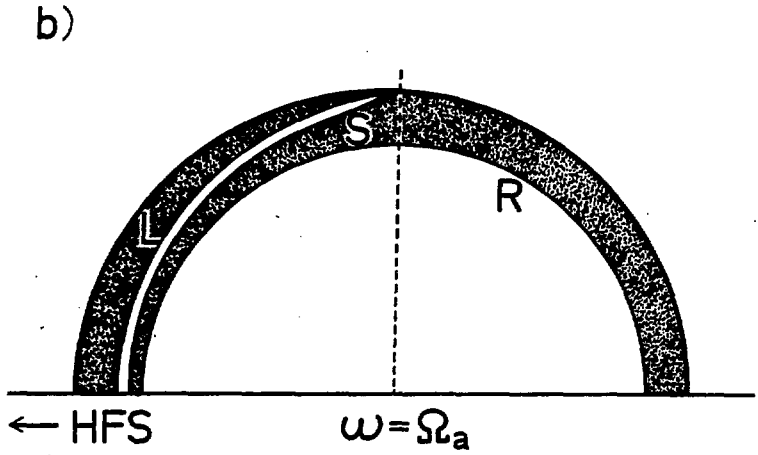

FIG.1(b)

c)

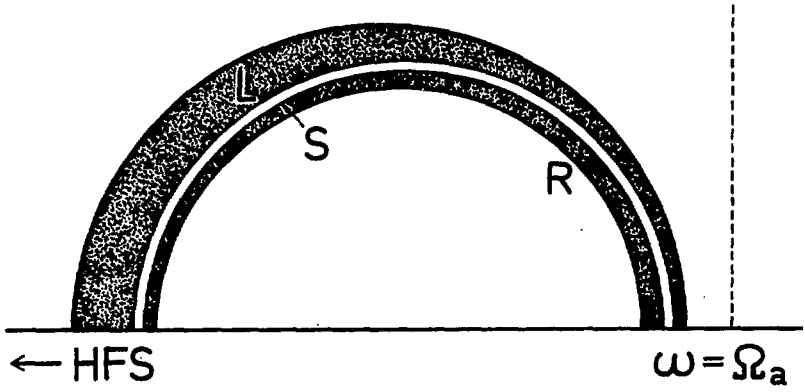

FIG.1(c)

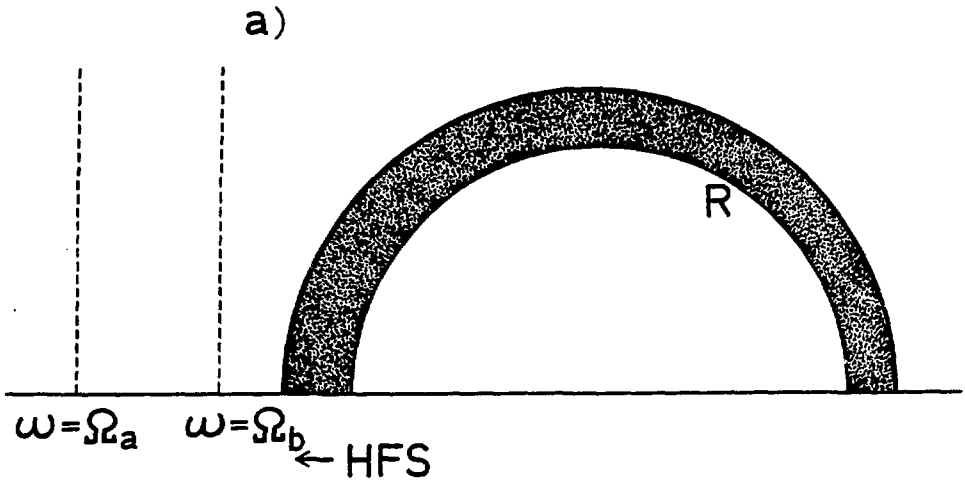
a)
R
$\omega=\Omega_a$
$\omega=\Omega_b$
← HFS

FIG.2(a)

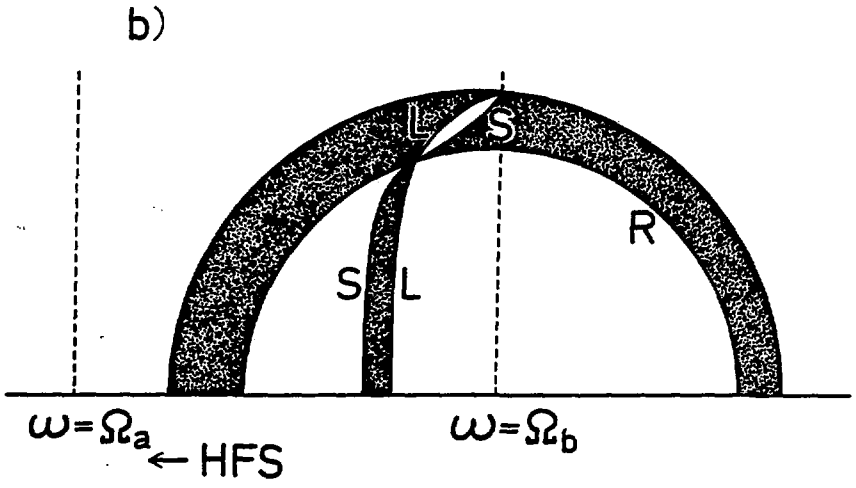
b)
L
S
R
S
L
$\omega=\Omega_a$
← HFS
$\omega=\Omega_b$

FIG.2(b)

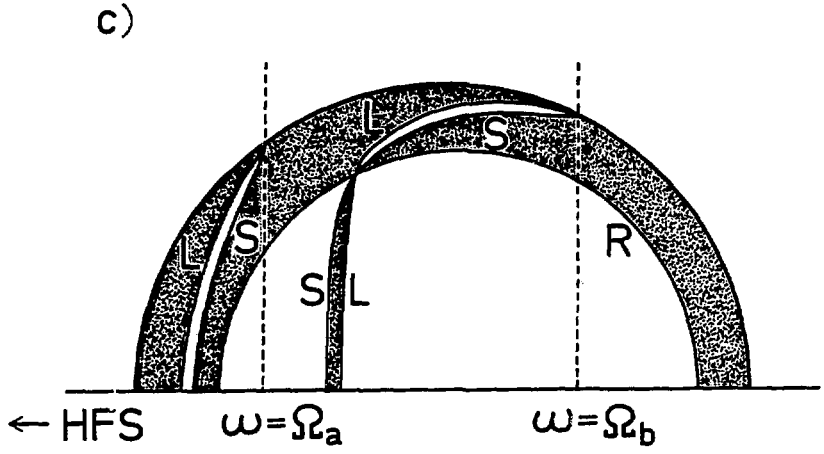

FIG.2(c)

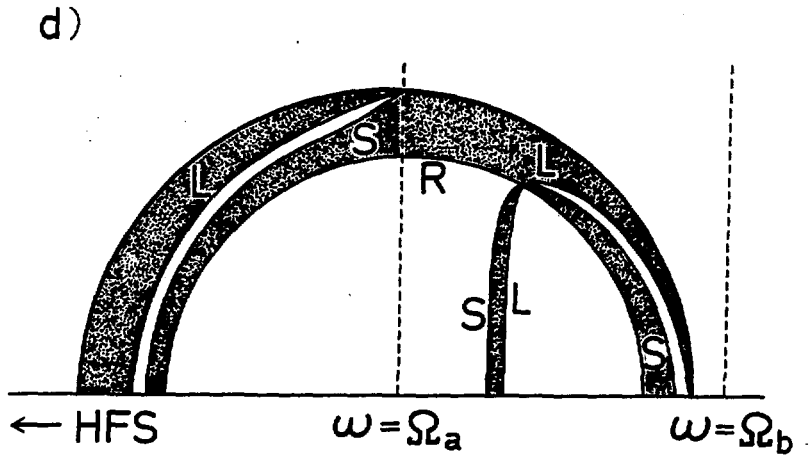

FIG.2(d)

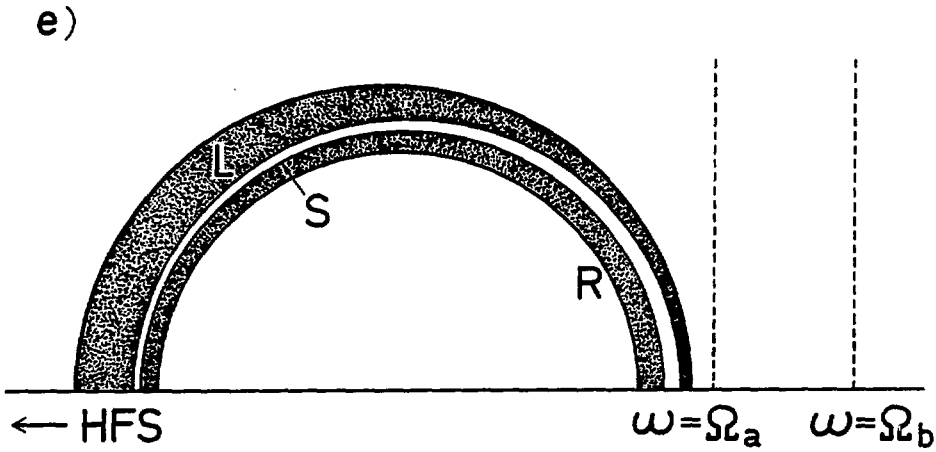

FIG.2(e)

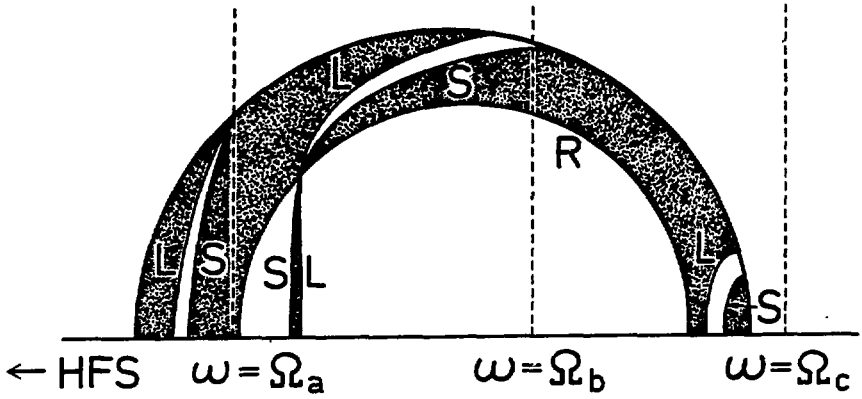

FIG.3

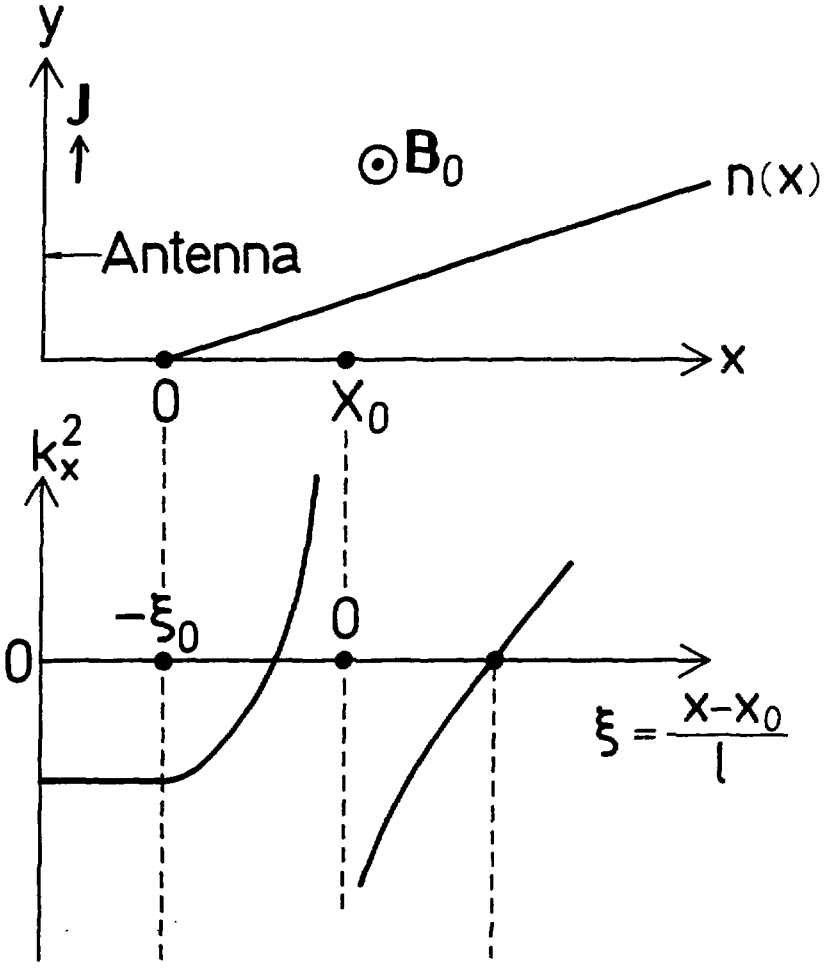

FIG.4

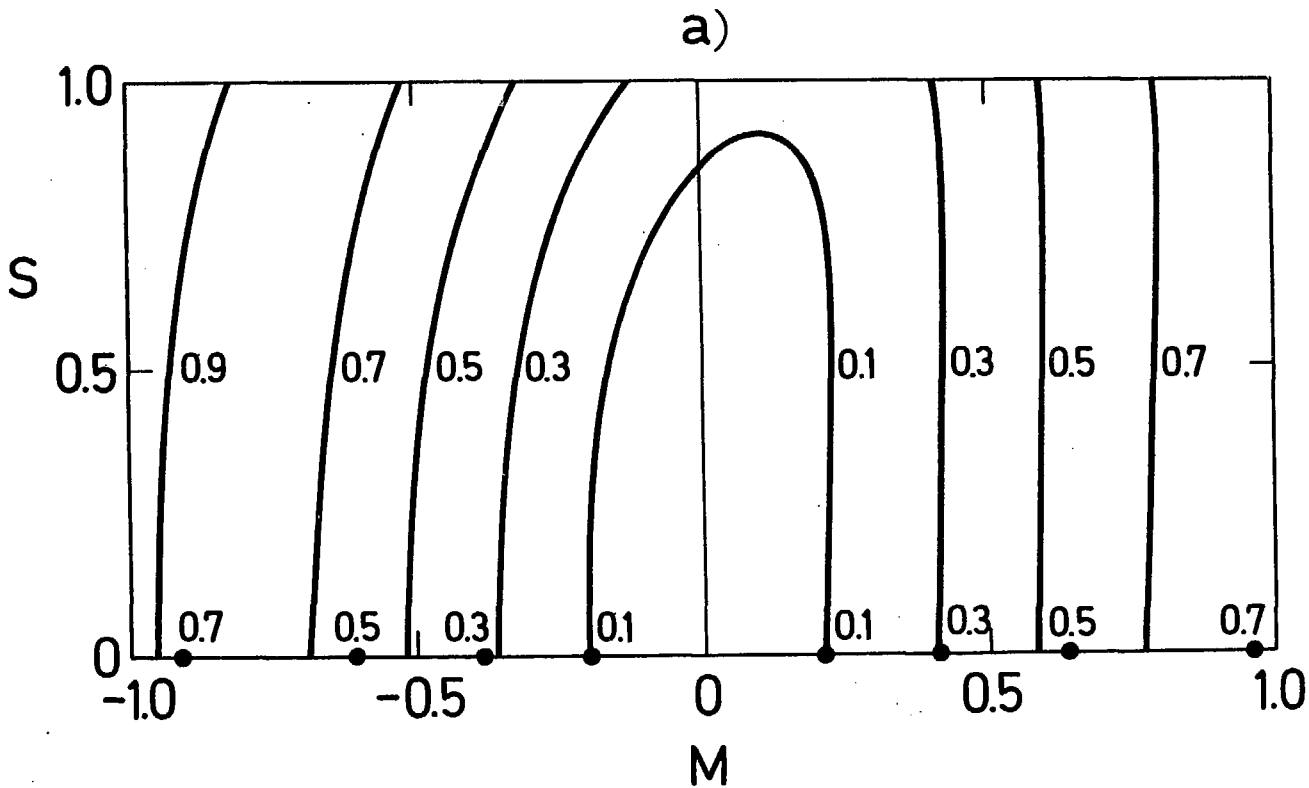

FIG.5(a)

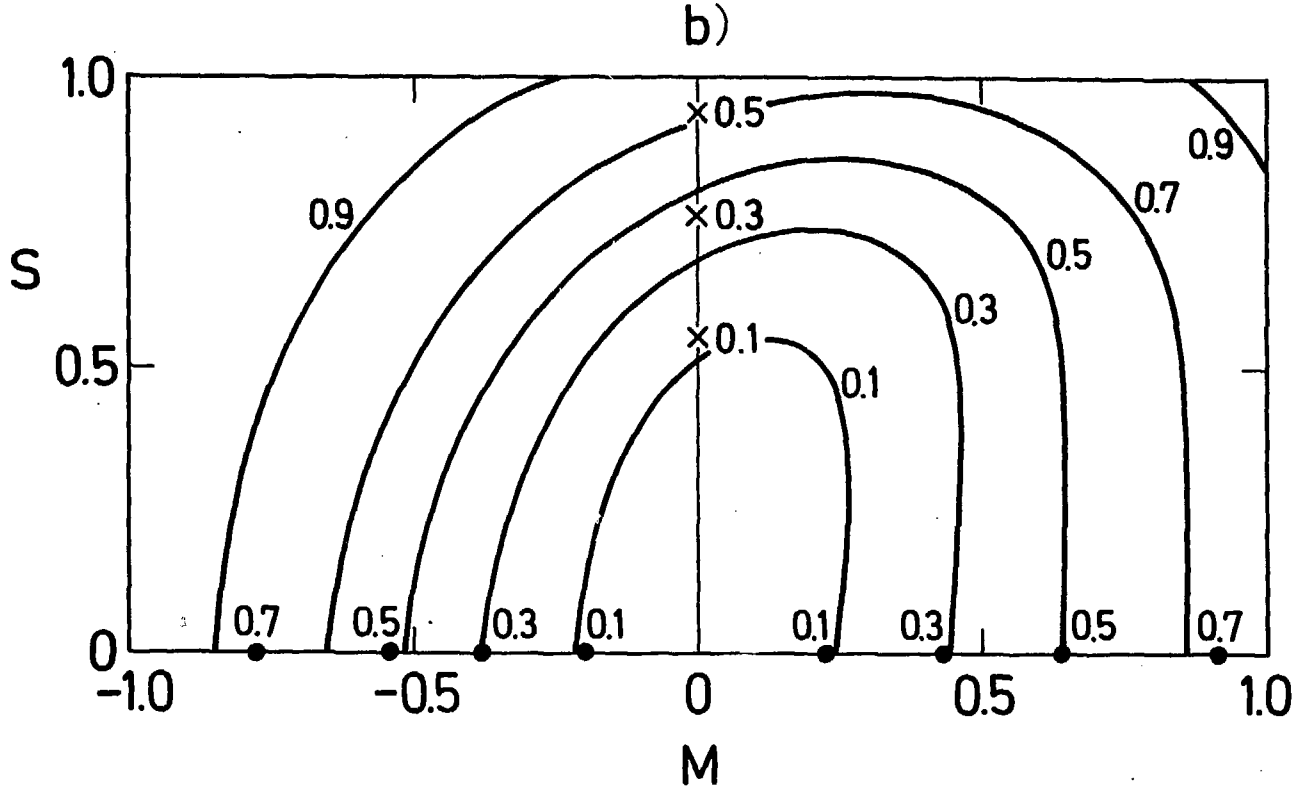
b)
1.0
0.5
0
S
-1.0
-0.5
0
0.5
1.0
M
0.5
0.3
0.1
0.9
0.7
0.5
0.3
0.1
0.9
0.7
0.5
0.3
0.1
0.1
0.3
0.5
0.7

FIG.5(b)

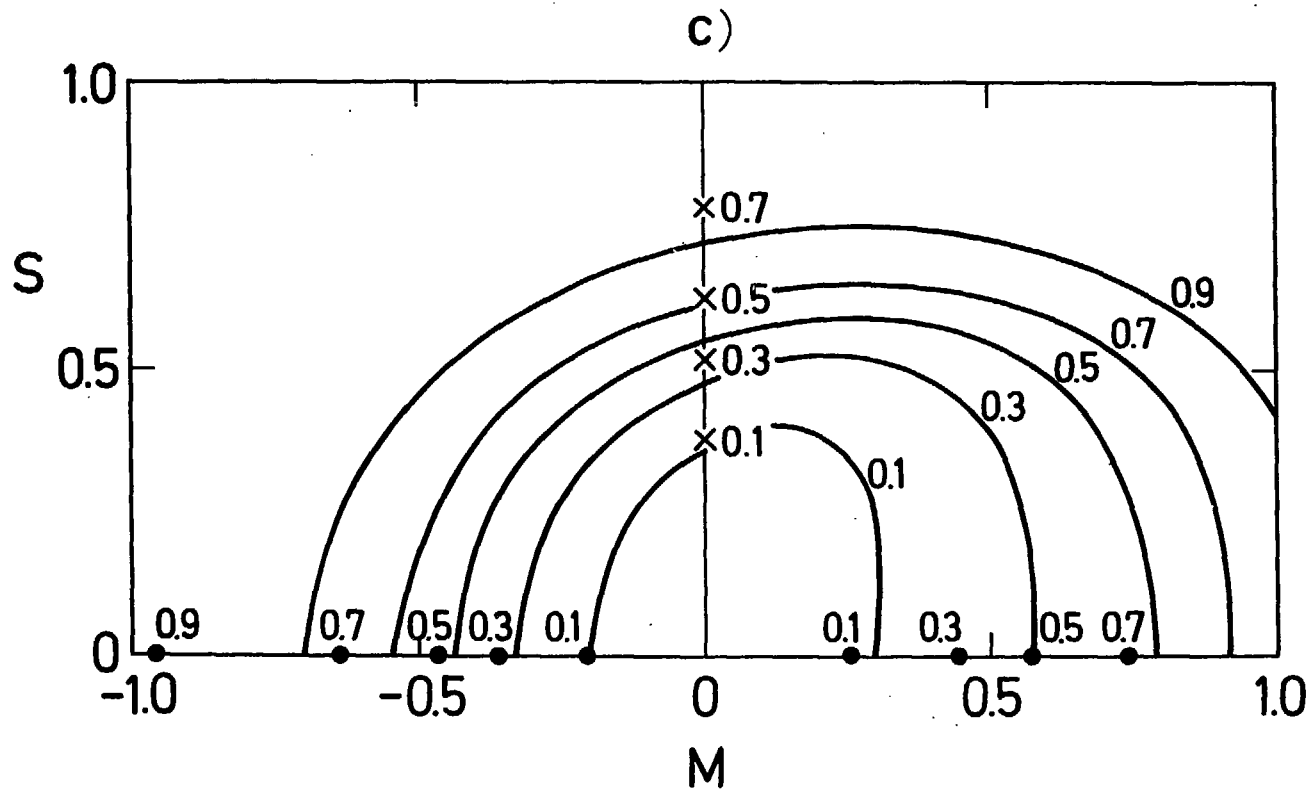
c)
1.0
S
0.5
0
-1.0
-0.5
0
0.5
1.0
M
0.7
0.5
0.3
0.1
0.9
0.7
0.5
0.3
0.1
0.9
0.7
0.5
0.3
0.1
0.1
0.3
0.5
0.7

FIG.5(c)

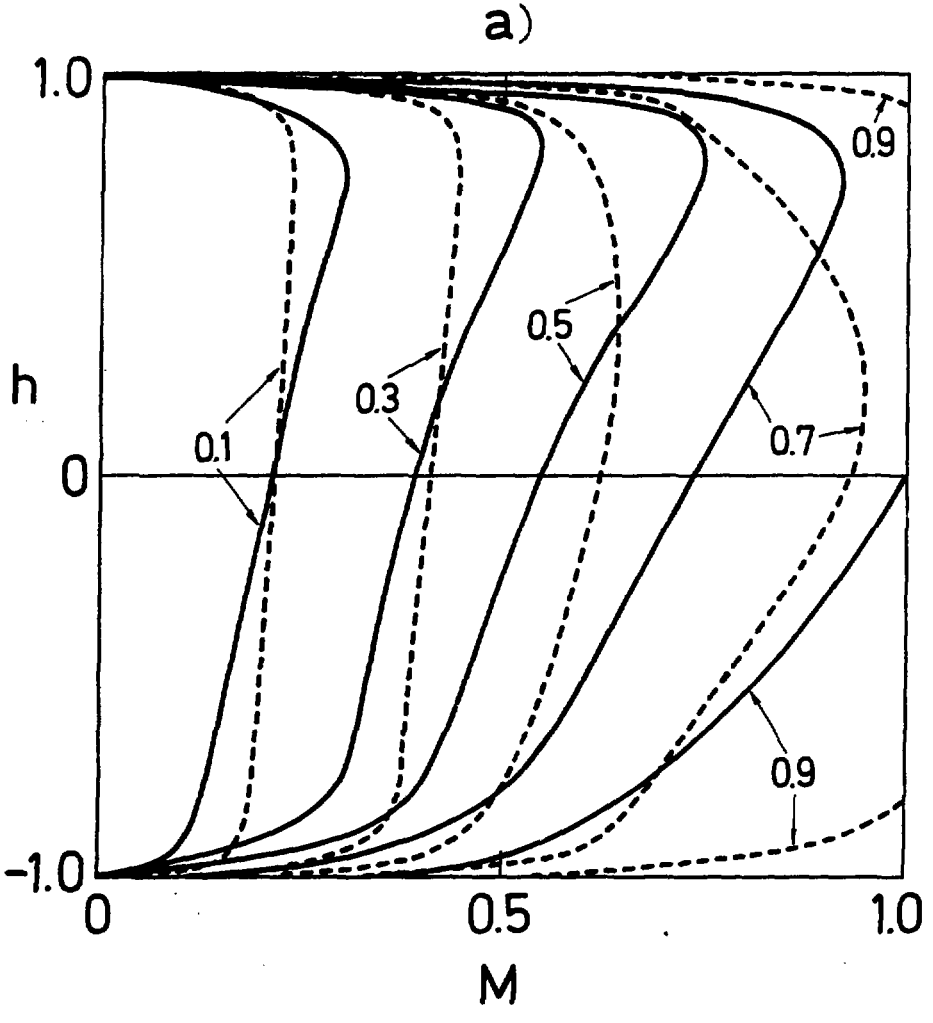

FIG.6(a)

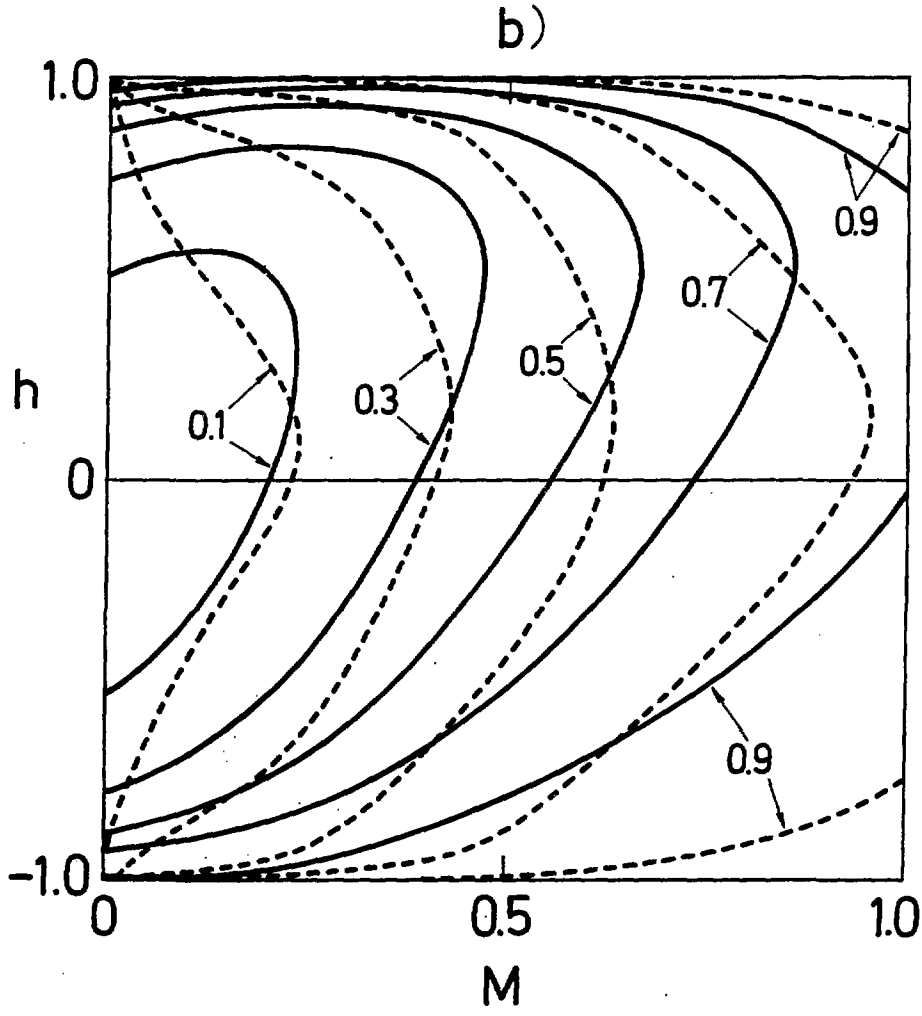

FIG.6(b)

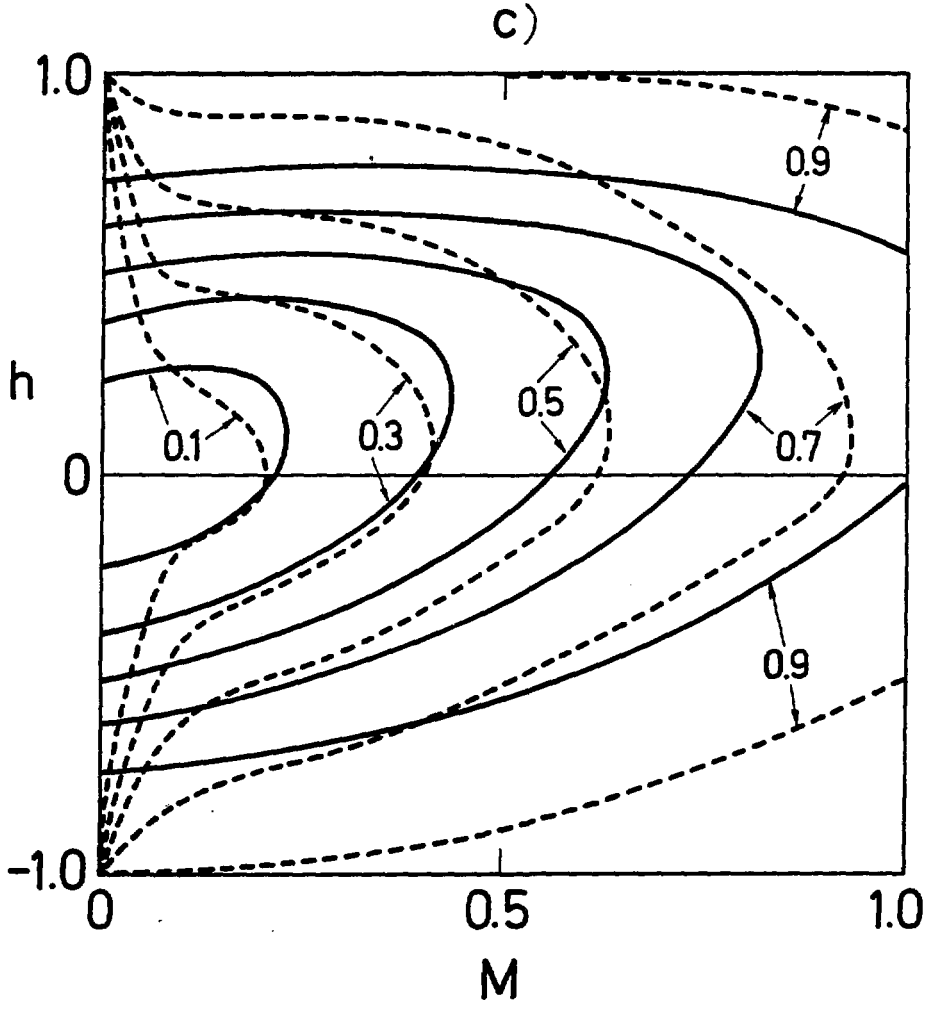

FIG.6(c)